NUMERICAL SOLUTION OF THE HEAT ADVECTION EQUATION IN A TWO-DIMENSIONAL DOMAIN USING THE DISCONTINUOUS GALERKIN METHOD

Ewa Węgrzyn-Skrzypczak

Department of Mathematics, Czestochowa University of Technology
Czestochowa, Poland
ewa.wegrzyn-skrzypczak@pcz.pl

Abstract. This paper presents a numerical solution of the heat advection equation in a two-dimensional domain using the Discontinuous Galerkin Method (DGM). The advection equation is widely used in heat transfer problems, particularly in the field of fluid dynamics. The discontinuous Galerkin method is a numerical technique that allows for the solution of partial differential equations using a piecewise polynomial approximation. In this study, DGM is applied to the heat advection equation and its effectiveness in solving the problem is investigated. The findings of this study suggest that the Discontinuous Galerkin Method is a promising approach for solving heat transfer problems in a two-dimensional domain.

1. Introduction

Heat advection is a term used to describe the process of heat transport by the movement of fluid without heat exchange with the environment or within the fluid. It belongs to the group of phenomena described by so called hyperbolic conservation laws. This is a phenomenon that occurs, for example, in the atmosphere or oceans and other fluid flows. In such a case, heat is transported along with the fluid flow, without exchanging heat with other objects or the environment. In the case of pure heat advection, the temperature inside the fluid changes due to changes in the flow velocity, which leads to the movement of temperature within the fluid.

Numerical methods are used to solve the heat advection equation. These methods involve discretizing the domain and the advection equation, which means breaking them down into smaller pieces or cells to simplify the problem. Once

discretized, appropriate numerical schemes are applied to find the temperature at successive time steps. The Finite Difference Method (FDM) is one such numerical method that approximates derivatives using difference equations [1]. The Finite Element Method (FEM) divides the domain into small elements and solves for the temperature within each element using polynomial approximations [2]. The Finite Volume Method (FVM) discretizes the domain into finite volumes and solves for the temperature fluxes between adjacent volumes [3]. The Discontinuous Galerkin Method (DGM) is a relatively new numerical technique that approximates solutions using piecewise polynomial functions [4-6]. Unlike the other methods, DGM allows for discontinuities in the approximations and is particularly effective at handling discontinuous or sharp features in the solution. DGM is a method that does not require continuity of the solution between elements. This is an advantage in problems with high gradients or solution jumps. For this reason, the DGM approach is potentially interesting for solving problems in various fields of mechanics where large inhomogeneities or material discontinuities occur [7, 8]. DGM involves approximating the solution using basis functions in each element and applying inter-element boundary conditions based on the Riemann or Lax-Friedrichs method.

The field of hyperbolic conservation laws has been extensively studied, with numerous research articles addressing various aspects of numerical methods and applications. LeVeque [9] provides a comprehensive overview of FVM specifically designed for hyperbolic problems, offering insights into the numerical treatment of conservation laws. Flaherty et al. [10] delve into the aspects of DGM for hyperbolic conservation laws. Chandrasekar [11] focuses on numerical methods in the context of atmospheric and oceanic sciences, shedding light on the specific challenges and techniques employed in these domains. The presented work focuses on a very detailed description of mathematical and numerical models.

2. Mathematical description of the problem

The problem concerns a two-dimensional domain denoted as Ω, filled with a fluid of temperature $T(x, y, t)$ and in motion. In this domain, a certain control subregion Ω' has been identified (Fig. 1).
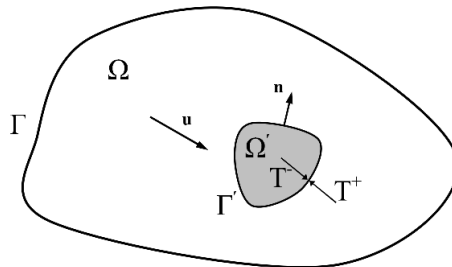

Fig. 1. The domain Ω with a designated control subdomain Ω'

The change of temperature T [K] on the boundary Γ' moving in the direction normal to Γ' can be written as an integral:

$$f = \int_{\Gamma'} -(\mathbf{u} \cdot \mathbf{n}) T ds, \tag{1}$$

where $\mathbf{u}$ is the velocity vector of fluid [m/s], while $\mathbf{n}$ is the vector normal to Γ'.

The value f of the integral (1) must be equal to the increase of temperature in time within the area Ω'. Based on this, one can write:

$$\frac{d}{dt} \int_{\Omega'} T dV = \int_{\Gamma'} -(\mathbf{u} \cdot \mathbf{n}) T ds. \tag{2}$$

Finally, equation (2) takes the form:

$$\frac{d}{dt} \int_{\Omega'} T dV = \int_{\Omega'} -\nabla \cdot (\mathbf{u} T) dV = \int_{\Omega'} -\left(u_x \frac{\partial T}{\partial x} + u_y \frac{\partial T}{\partial y} \right) dV. \tag{3}$$

The balance (3) for each control subregion Ω' is therefore as follows:

$$\int_{\Omega'} \left(\frac{dT}{dt} + u_x \frac{\partial T}{\partial x} + u_y \frac{\partial T}{\partial y} \right) dV = 0. \tag{4}$$

Assuming the continuity of the temperature field, the advection heat differential equation in a two-dimensional domain takes the form:

$$\frac{\partial T}{\partial t} + u_x \frac{\partial T}{\partial x} + u_y \frac{\partial T}{\partial y} = 0, \tag{5}$$

where x, y [m] are the spatial coordinates of the Cartesian coordinate system, while u_x, u_y [m/s] are the components of the heat advection velocity vector in the direction of x and y axes, respectively.

2.1. Formulation of the Discontinous Galerkin Method

For the needs of the DG method, the concept of a two-dimensional space of polynomials of not higher than p-th degree was introduced:

$$P^p(\Omega') = \left\langle x^a y^b \right\rangle_{0 \leq a+b \leq p}. \tag{6}$$

It is necessary to find $T \in P^p(\Omega')$ such that for every $w \in P^p(\Omega')$ it is satisfied:

$$\int_{\Omega'} w\left(\frac{dT}{dt} + u_x \frac{\partial T}{\partial x} + u_y \frac{\partial T}{\partial y} \right) dV + \int_{\Gamma'} w\left(\frac{\tau^- - |\tau^-|}{2} \right)[T]\,ds = 0, \qquad (7)$$

where w is a certain weight function, $\tau^- = \mathbf{u} \cdot \mathbf{n}$, while $[T] = T^+ - T^-$ (Fig. 2). The expression $\left(\dfrac{\tau^- - |\tau^-|}{2} \right)[T]$ in equation (7) is defined as the flux measure according to Lax-Friedrichs.
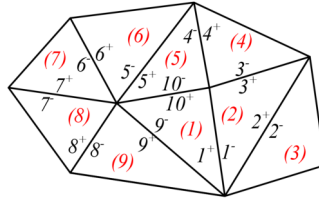

Fig. 2. Example division of the area with numbered shared edges

The solution of equation (7) is local and applies to a designated control domain Ω'. In the case of two dimensions, there are several possibilities for dividing the domain Ω into elementary subdomains Ω' called finite elements. In the considered case, triangular elements were chosen. An example domain division is shown in Figure 2. In the DG method, it is not necessary to know the connections between the vertex nodes of the elements; it is enough to have information about the connections between the edges. It is convenient to assign a unique index to each edge and use + or – to determine whether it belongs to a given element.
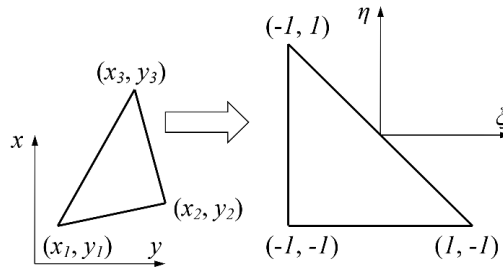

Fig. 3. Normalization of a triangular finite element

In Figure 3, the reference triangle is shown in the real coordinates x and y, as well as in the normalized coordinates ξ, η. The transformations are expressed as follows:

$$\begin{pmatrix} x \\ y \end{pmatrix} = -\frac{\xi + \eta}{2}\begin{pmatrix} x_1 \\ y_1 \end{pmatrix} + \frac{1 + \xi}{2}\begin{pmatrix} x_2 \\ y_2 \end{pmatrix} + \frac{1 + \eta}{2}\begin{pmatrix} x_3 \\ y_3 \end{pmatrix}. \qquad (8)$$

The next step in the described method is to construct an orthogonal basis of approximation polynomials for the triangular finite element. Koornwinder proposed the Jacobi polynomial products as the approximation functions [12]. The polynomial of order n is additionally parameterized by real coefficients α, β:

$$P_n^{\alpha,\beta}(x) = \frac{1}{(-1)^n 2^n n!(1-x)^\alpha (1+x)^\beta} \frac{d^n}{dx^n}\left\{(1-x)^\alpha (1+x)^\beta (1-x^2)^n\right\}. \qquad (9)$$

For integer values of α, β, the Jacobi polynomials are mutually orthogonal:

$$\int_{-1}^{1}\left(\frac{1-x}{2}\right)^\alpha \left(\frac{1+x}{2}\right)^\beta P_n^{\alpha,\beta}(x) P_m^{\alpha,\beta}(x)\,dx = \delta_{nm} \frac{2}{2n+\alpha+\beta+1} \frac{(n+\alpha)!(n+\beta)!}{n!(n+\alpha+\beta)!}. \quad (10)$$

When $\alpha = \beta = 0$, the Jacobi polynomial reduces to the Legendre polynomial:

$$P_n^{0,0}(x) = L_n(x), \qquad (11)$$

Basic properties of Jacobi polynomials are as follows:

$$P_n^{\alpha,\beta}(1) = \frac{(n+\alpha)!}{n!\alpha!}, \qquad (12)$$

$$P_n^{\alpha,\beta}(-x) = (-1)^n P_n^{\beta,\alpha}(-x). \qquad (13)$$

The form (9) is inconvenient from the point of view of computational practice. The following recursive formula is more convenient in this case:

$$
\begin{aligned}
&P_0^{\alpha,\beta}(x) = 0, \\
&P_1^{\alpha,\beta}(x) = \alpha + 1 + \frac{(\alpha+\beta+2)(x-1)}{2} \\
&2(n+1)(n+\alpha+\beta+1)(2n+\alpha+\beta)P_{n+1}^{\alpha,\beta}(x) = \\
&= \left\{(2n+\alpha+\beta+1)(\alpha^2-\beta^2) + x\frac{(2n+\alpha+\beta+2)!}{(2n+\alpha+\beta-1)!}\right\} P_n^{\alpha,\beta}(x) + \\
&- 2(n+\alpha)(n+\beta)(2n+\alpha+\beta+2)P_{n-1}^{\alpha,\beta}(x).
\end{aligned}
\qquad (14)
$$

Returning to the construction of the basis of orthogonal polynomials for a triangle, it is necessary to perform a mapping procedure from the triangle to a square. This is done by introducing new coordinates, a and b:

$$
\begin{aligned}
a &= \frac{2(1+\xi)}{1-\eta} - 1, \\
b &= \eta.
\end{aligned}
\qquad (15)
$$

The basis of orthogonal functions ϕ_{nm} then takes the form:

$$\phi_{nm}(a,b) = P_n^{0,0}(a)\left(\frac{1-b}{2}\right)^n P_m^{2n+1,0}(b), \tag{16}$$

or by substituting (15) into (16):

$$\phi_{nm}(\xi,\eta) = P_n^{0,0}\left(\frac{2(1+\xi)}{1-\eta}-1\right)\left(\frac{1-\eta}{2}\right)^n P_m^{2n+1,0}(\eta). \tag{17}$$

The functions (17) are mutually orthogonal because:

$$\int_{-1}^{1}\int_{-1}^{-\eta}\phi_{ij}\,\phi_{kl}\,d\xi\,d\eta = \delta_{ik}\,\delta_{il}\,\frac{1}{(i+0.5)(i+j+1)}. \tag{18}$$

The form of the interpolating polynomial for any function whose values at the nodes are known is given as follows:

$$f(\xi,\eta) = \sum_{i=0}^{i=p}\sum_{j=0}^{j=p-i}\phi_{ij}(\xi,\eta)\,\hat{f}_{ij}, \tag{19}$$

where p is the degree of approximation, $\hat{f}_{ij}$ are the coefficients of the function expansion at the given node.

There is a relationship between the degree of approximation p and the number M of internal nodes in the finite element. In the case of a triangle, this relationship can be expressed as follows:

$$M = \frac{(p+1)(p+2)}{2}. \tag{20}$$

Figure 4 shows examples of the distribution of internal nodes in a triangular finite element depending on the order of approximation.
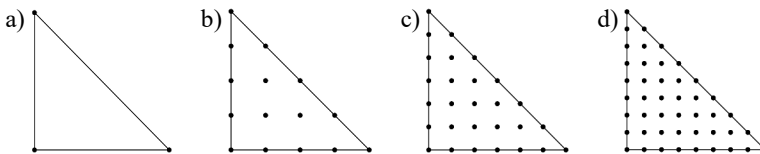

Fig. 4. Different ways of distributing nodes in a triangular finite element for $p = 1$ (a), $p = 4$ (b), $p = 6$ (c), $p = 8$ (d)

Having a set of M nodes located inside the element and using the functions (17), for convenience of further considerations, the Vandermonde matrix $\mathbf{V}$ was constructed, whose coefficients take the value:

$$V_{nij} = \phi_{ij}\left(\xi_n, \eta_n\right). \tag{21}$$

The values of $f\left(\xi_n, \eta_n\right)$, where n denotes the node index, are calculated as follows:

$$f\left(\xi_n, \eta_n\right) = \sum_{i=0}^{i=p} \sum_{j=0}^{j=p-i} V_{nij}\hat{f}_{ij} = \sum_{m=1}^{m=M} V_{nm}\hat{f}_m, \tag{22}$$

where m specifies the successive combinations of indices ij, where the number of combinations is equal to the number of nodes.

The value of the expansion coefficient of the interpolating function at the n-th node can be calculated using the coefficients of inverse Vandermonde matrix:

$$\hat{f}_n = \sum_{m=1}^{m=M} \left(V^{-1}\right)_{nm} f\left(\xi_m, \eta_m\right). \tag{23}$$

The partial derivatives of f with respect to ξ and η are calculated as follows:

$$\frac{\partial f}{\partial \xi}\left(\xi, \eta\right) = \sum_{i=0}^{i=p} \sum_{j=0}^{j=p-i} \frac{\partial \varphi_{ij}}{\partial \xi}\left(\xi, \eta\right)\hat{f}_{ij}, \tag{24}$$

$$\frac{\partial f}{\partial \eta}\left(\xi, \eta\right) = \sum_{i=0}^{i=p} \sum_{j=0}^{j=p-i} \frac{\partial \varphi_{ij}}{\partial \eta}\left(\xi, \eta\right)\hat{f}_{ij}. \tag{25}$$

Knowing that:

$$\frac{dP_n^{\alpha,\beta}}{dx} = \left(\frac{n+\alpha+\beta+1}{2}\right)P_{n-1}^{\alpha+1,\beta+1}(x), \tag{26}$$

the derivatives of (17) with respect to ξ and η can be calculated in the following way:

$$\frac{\partial \varphi_{nm}}{\partial \xi}\left(\xi, \eta\right) = \left(\frac{2}{1-\eta}\right)\left(\frac{n+1}{2}\right)P_{n-1}^{1,1}\left(\frac{2(1+\xi)}{1-\eta}-1\right)\left(\frac{1-\eta}{2}\right)^n P_m^{2n+1,0}(\eta), \tag{27}$$

$$\frac{\partial \varphi_{nm}}{\partial \eta}\left(\xi, \eta\right) = \left\{\frac{2}{\left(1-\eta\right)^2}\left(\frac{n+1}{2}\right)P_{n-1}^{1,1}\left(\frac{2(1+\xi)}{1-\eta}-1\right)\right\}\left(\frac{1-\eta}{2}\right)^n P_m^{2n+1,0}(\eta) +$$

$$+ P_n^{0,0}\left(\frac{2(1+\xi)}{1-\eta}-1\right)\left\{-\frac{n}{2}\left(\frac{1-\eta}{2}\right)^{n-1}\right\}P_m^{2n+1,0}(\eta) + \tag{28}$$

$$+ P_n^{0,0}\left(\frac{2(1+\xi)}{1-\eta}-1\right)\left(\frac{1-\eta}{2}\right)^n \left\{\frac{m+2n+2}{2} P_{m-1}^{2n+2,1}(\eta)\right\}.$$

Derivatives (27) and (28) for each node in the element and all combinations can be conveniently stored as matrix elements:

$$\hat{D}_{nm}^{\xi} = \frac{\partial \varphi_m}{\partial \xi}(\xi_n, \eta_n), \tag{29}$$

$$\hat{D}_{nm}^{\eta} = \frac{\partial \varphi_m}{\partial \eta}(\xi_n, \eta_n). \tag{30}$$

Using (23) and (29), (30), the derivatives (24) and (25) are written in the following form:

$$\frac{\partial f}{\partial \xi}(\xi_n, \eta_n) = \sum_{m=1}^{m=M} \hat{D}_{nm}^{\xi} \hat{f}_m, \tag{31}$$

$$\frac{\partial f}{\partial \eta}(\xi_n, \eta_n) = \sum_{m=1}^{m=M} \hat{D}_{nm}^{\eta} \hat{f}_m. \tag{32}$$

Finally, by substituting $\mathbf{D}^{\xi} = \hat{\mathbf{D}}^{\xi} \mathbf{V}^{-1}$ and $\mathbf{D}^{\eta} = \hat{\mathbf{D}}^{\eta} \mathbf{V}^{-1}$ into (31) and (32), they take the form:

$$\frac{\partial f}{\partial \xi} = \mathbf{D}^{\xi} \mathbf{f}, \tag{33}$$

$$\frac{\partial f}{\partial \eta} = \mathbf{D}^{\eta} \mathbf{f}. \tag{34}$$

The weak form of the advection equation (7) can be written in the following form:

$$\sum_{m=1}^{m=M} \left\{ \int_{\Omega'} h_n h_m dV \frac{dT_m}{dt} \right\} + \sum_{m=1}^{m=M} \left\{ \int_{\Omega'} u h_n \frac{\partial h_m}{\partial x} dV T_m \right\} +$$
$$+ \sum_{m=1}^{m=M} \left\{ \int_{\Omega'} v h_n \frac{\partial h_m}{\partial y} dV T_m \right\} + \int_{\Gamma'} \left\{ h_n \left(\frac{\tau^- - |\tau^-|}{2} \right) [T] \right\} ds = 0. \tag{35}$$

Substituting $h_n = f(\xi, \eta)$, $h_m = g(\xi, \eta)$, one can expand the integrals in equation (35) as follows:

$$\int_{\Omega'} h_n h_m dV = \frac{\partial(x,y)}{\partial(\xi,\eta)} \int_{-1}^{1} \int_{-1}^{-\eta} f(\xi,\eta) g(\xi,\eta) d\xi d\eta, \tag{36}$$

$$\int_{\Omega'} h_n \frac{\partial h_m}{\partial x} dV = \frac{\partial(x,y)}{\partial(\xi,\eta)} \frac{\partial \xi}{\partial x} \int_{-1}^{1} \int_{-1}^{-\eta} f(\xi,\eta) \frac{\partial g}{\partial \xi}(\xi,\eta) d\xi d\eta +$$

$$+ \frac{\partial(x,y)}{\partial(\xi,\eta)} \frac{\partial \eta}{\partial x} \int_{-1}^{1} \int_{-1}^{-\eta} f(\xi,\eta) \frac{\partial g}{\partial \eta}(\xi,\eta) d\xi d\eta, \tag{37}$$

$$\int_{\Omega'} h_n \frac{\partial h_m}{\partial y} dV = \frac{\partial(x,y)}{\partial(\xi,\eta)} \frac{\partial \xi}{\partial y} \int_{-1}^{1} \int_{-1}^{-\eta} f(\xi,\eta) \frac{\partial g}{\partial \xi}(\xi,\eta) d\xi d\eta +$$

$$+ \frac{\partial(x,y)}{\partial(\xi,\eta)} \frac{\partial \eta}{\partial y} \int_{-1}^{1} \int_{-1}^{-\eta} f(\xi,\eta) \frac{\partial g}{\partial \eta}(\xi,\eta) d\xi d\eta. \tag{38}$$

Using the relation (19) for the integral (36), one can obtain:

$$\frac{\partial(x,y)}{\partial(\xi,\eta)} \int_{-1}^{1} \int_{-1}^{-\eta} f(\xi,\eta) g(\xi,\eta) d\xi d\eta =$$

$$= \frac{\partial(x,y)}{\partial(\xi,\eta)} \int_{-1}^{1} \int_{-1}^{-\eta} \left\{ \sum_{m=1}^{m=M} \hat{f}_m \varphi_m(\xi,\eta) \right\} \left\{ \sum_{n=1}^{n=M} \hat{g}_n \varphi_n(\xi,\eta) \right\} d\xi d\eta =$$

$$= \frac{\partial(x,y)}{\partial(\xi,\eta)} \sum_{m=1}^{m=M} \sum_{n=1}^{n=M} \hat{f}_m \hat{g}_n \int_{-1}^{1} \int_{-1}^{-\eta} \varphi_m(\xi,\eta) \varphi_n(\xi,\eta) d\xi d\eta =$$

$$= \frac{\partial(x,y)}{\partial(\xi,\eta)} \sum_{m=1}^{m=M} \sum_{n=1}^{n=M} \hat{f}_m \hat{g}_n \delta_{nm} C_n = \frac{\partial(x,y)}{\partial(\xi,\eta)} \sum_{n=1}^{n=M} \hat{f}_m \hat{g}_n C_n. \tag{39}$$

The elements C_n of diagonal matrix arise from the orthogonality condition (10) of the applied polynomials. The mass matrix is obtained by computing the integrals in equation (39) using the known values of f and g at the element nodes to compute $\hat{f}$, $\hat{g}$. The resulting mass matrix is given by:

$$\frac{\partial(x,y)}{\partial(\xi,\eta)} \sum_{n=1}^{n=M} \hat{f}_m \hat{g}_n C_n = \frac{\partial(x,y)}{\partial(\xi,\eta)} \left(\mathbf{V}^{-1} \mathbf{f} \right) \mathbf{C} \left(\mathbf{V}^{-1} \mathbf{g} \right) = \mathbf{f}^t \mathbf{M} \mathbf{g}, \tag{40}$$

where $\mathbf{M} = \left(\mathbf{V}^{-1} \right)^t \mathbf{C} \left(\mathbf{V}^{-1} \right)$. By assuming again that $f = h_n(\xi,\eta)$, $g = h_m(\xi,\eta)$, and $h_n(\xi_m, \eta_m) = \delta_{nm}$, one obtains:

$$\int_{\Omega'} h_n h_m dV = \mathbf{h}_n^t \mathbf{M} \mathbf{h}_m = \frac{\partial(x,y)}{\partial(\xi,\eta)} \sum_{k=1}^{k=M} \sum_{j=1}^{j=M} h_n\left(\xi_j,\eta_j\right) M_{jk} h_m\left(\xi_k,\eta_k\right) =$$

$$= \frac{\partial(x,y)}{\partial(\xi,\eta)} \sum_{k=1}^{k=M} \sum_{j=1}^{j=M} \delta_{nj} M_{jk} \delta_{km} = \frac{\partial(x,y)}{\partial(\xi,\eta)} \mathbf{M}_{nm}, \tag{41}$$

$$\int_{\Omega'} h_n \frac{\partial h_m}{\partial x} dV = \left\{ \frac{\partial(x,y)}{\partial(\xi,\eta)} \frac{\partial \xi}{\partial x} \right\} \left(\mathbf{MD}^\xi\right)_{nm} + \left\{ \frac{\partial(x,y)}{\partial(\xi,\eta)} \frac{\partial \eta}{\partial x} \right\} \left(\mathbf{MD}^\eta\right)_{nm} = D_{nm}^x, \tag{42}$$

$$\int_{\Omega'} h_n \frac{\partial h_m}{\partial y} dV = \left\{ \frac{\partial(x,y)}{\partial(\xi,\eta)} \frac{\partial \xi}{\partial y} \right\} \left(\mathbf{MD}^\xi\right)_{nm} + \left\{ \frac{\partial(x,y)}{\partial(\xi,\eta)} \frac{\partial \eta}{\partial y} \right\} \left(\mathbf{MD}^\eta\right)_{nm} = D_{nm}^y. \tag{43}$$

To calculate the integral over the element boundary:

$$\int_{\Gamma'} \left\{ h_n \left(\frac{\tau^- - |\tau^-|}{2} \right) [T] \right\} ds = \sum_{m=1}^{m=M} \sum_{e=1}^{e=3} \int_{\Gamma'} h_n h_m \, ds \left(\frac{\tau^- - |\tau^-|}{2} \right) [T]. \tag{44}$$

Assuming that:

$$\phi_{ij} = \sum_{n=1}^{n=M} \phi_{ij}\left(\xi_n,\eta_n\right) h_n\left(\xi,\eta\right). \tag{45}$$

One can obtain:

$$h_n\left(\xi,\eta\right) = \sum_{i=0}^{i=p} \sum_{j=0}^{j=p-i} \left(V^{-1}\right)_{nij} \varphi_{ij}. \tag{46}$$

For each edge of the element, the integral in expression (44) can be calculated as follows:

$$\int_{\Gamma'} h_n h_m \, ds \sum_{i=0}^{i=p} \sum_{j=0}^{j=p-i} \sum_{l=0}^{l=p-i} \left(V^{-1}\right)_{nij} \left(V^{-1}\right)_{nil} P_j^{2i+1,0}\left(-1\right) P_l^{2i+1,0}\left(-1\right) \frac{2}{2i+1}. \tag{47}$$

3. Example of calculations

Test calculations were carried out in a square area with a side length of 3 m. The area was divided into 72 triangular finite elements. The calculations used an 8th order approximation and a 4th order Runge-Kutta scheme. In the area, a temperature field was generated described by the equation $T(x,y) = 300 e^{-x^2} e^{-y^2}$ (Fig. 6a).

Table 1. Coefficients for the Runge-Kutta 4th-order scheme

No.	RK4a	RK4b	RK4c
0	0	0.1496590219992291	0
1	−0.4178904744998519	0.3792103129996273	0.1496590219992291
2	−1.192151694642677	0.8229550293869817	0.3704009573642048
3	−1.697784692471528	0.6994504559491221	0.6222557631344432
4	−1.514183444257156	0.153057247968152	0.9582821306746903

According to Runge-Kutta, scheme solution $T(t + \Delta t)$ is obtained as follows:
1. $RK_t = t + RK4c[i]\,\Delta t$
2. $\Delta \mathbf{T} = RK4a[i] + \Delta t\,(-\mathbf{u}_x \cdot \mathbf{D}^x \mathbf{T} - \mathbf{u}_y \cdot \mathbf{D}^y \mathbf{T} - \text{Flux})$
3. $\mathbf{T} = \mathbf{T} + RK4b[i]\,\Delta \mathbf{T}$
4. $i = i + 1$
5. if $i < 5$ return to 1

Two calculation variants were carried out (Fig. 5). In the first case, the temperature field was advected parallel to the x-axis, while in the second case, advection occurred at a 45-degree angle to the x-axis. The time step of $\Delta t = 0.01$ s was used for the calculations. The total time was 3 s. The initial temperature field as well as the temporary fields for both cases are shown in Figure 6. The temperature distributions after 3 s (Fig. 6b-c) show very good agreement with introduced velocity field.
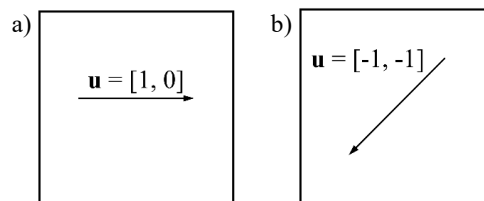

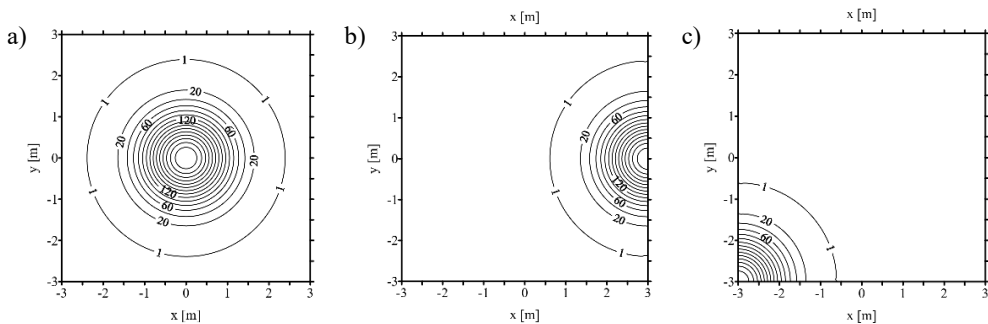Fig. 5. Advection velocity in two calculation variants

Fig. 6. Initial temperature distribution (a), temperature field at $\mathbf{u} = [1, 0]$ after $t = 3$ s (b), temperature field at $\mathbf{u} = [–1, –1]$ after $t = 3$ s (c)

4. Conclusions

A mathematical and numerical description of the two-dimensional pure heat advection process using the DG method was presented. Only local operations were performed on the right hand side of equation, which leads to small and dense matrices. Each element can have a different size and polynomial order, which enables local adaptation and facilitates hp-adaptivity. Numerical integration is not required, and the main computation is done elementwise – this is suitable for parallel computing. The drawback of the DG method is that it increases the total number of degrees of freedom compared to the classical FEM. The findings of this study hold practical applicability across a range of fields, including atmospheric and oceanic sciences, engineering, and computational physics. These insights have the potential to contribute to advancements and improvements in various real-world applications.

References

[1]   Dimov, I., Farago, I., & Vulkov, L. (2015). *Finite Difference Methods, Theory and Applications*. Springer-Verlag GmbH.

[2]   Whiteley, J. (2017). *Finite Element Methods: A Practical Guide*. Springer Int. Pub. AG.

[3]   Maliska, C. (2023). *The Finite Volume Method*. DOI: 10.1007/978-3-031-18235-8_3.

[4]   Reed, W.H., & Hill, T.R. (1973). *Triangular Mesh Methods for the Neutron Transport Equation*. Technical report LA-UR-73-479, Los Alamos National Laboratory. Los Alamos.

[5]   Lesaint, P., & Raviart, A. (1974). *On a Finite Element Method for Solving the Neutron Transport Equation*, in: *Mathematical Aspects of Finite Elements in Partial Differential Equations*. C.A. deBoor. New York: Academic Press, 89-123.

[6]   Dolejší, V., & Feistauer, M. (2015). *Discontinuous Galerkin Method: Analysis and Applications to Compressible Flow*. Cham: Springer.

[7]   Pozorski, Z., & Pozorska, J. (2022). Influence of the heterogeneity of the core material on the local instability of a sandwich panel. *Materials 2022*, *15*(19), 6687. DOI: 10.3390/ma15196687

[8]   Pozorska, J. (2018). Numerical modelling of sandwich panels with a non-continuous soft core. MATEC Web Conf., 157, 06007. DOI: 10.1051/matecconf/201815706007

[9]   LeVeque, R.J. (2012). *Finite Volume Methods for Hyperbolic Problems*. Cambridge University Press.

[10] Flaherty, J.E., Krivodonova, L., Remacle, J.-F., & Shephard, M.S. (2002), Aspects of discontinuous Galerkin methods for hyperbolic conservation laws. *Element Analysis and Design*, *38*(10), 889-908.

[11] Chandrasekar, A. (2022), *Numerical Methods for Atmospheric and Oceanic Sciences*. Cambridge University Press.

[12] Koornwinder, T.H. (1984). Orthogonal polynomials with weight function $(1-x)\alpha(1+x)\beta+M\delta(x+1)+N\delta(x-1)$. *Canadian Mathematical Bulletin*, *27*(2), 205-214.